DTU Compute
Institut for Matematik og Computer Science

Danmarks Tekniske Universitet

Bachelor's project

Geodesic circle packing on 2D surfaces

s183529 - Jonas Søeborg Nielsen

May 16, 2022

Preface

The work in this project has been performed exclusively by Jonas Søeborg Nielsen, student s183529 at Technical University of Denmark (DTU), as a final Bachelor's project. The project process has been guided by Steen Markvorsen[1] and David Brander[2], DTU compute. All `Python` implementations written in the project can be be found in the `GitHub` repository linked below.

GitHub repository link
https://github.com/MEGAjosni/DTU_s183529_Bachelors_project.git

Abstract

This report is concerned with the task of constructing geodesic circle packing's on 2D surfaces. The stepping stone is an algorithm used to make circle packing's within the plane, using tangent circle grow curves to expand the packing. Motivated by the task of using the algorithm to make circle packing's within other geometries than the plane, a more general definition of straight lines and circles on arbitrary 2D surfaces is explored, culminating in the concept of geodesics and geodesic circles within differential geometry. It was noticed that the difficulty of computing these measures analytically rises as the complexity of the geometry increases, thus 3 different methods have been used to handle different types of problems. In the simplest case, the geodesic equation has a somewhat simple analytic solution analogue to the case of the plane, which is the case of the cylinder. For some more complex geometries such as the sphere, there exist parametrizations that maps circles in the parameter domain to geodesic circles on the surface, which is the case of the stereographic projection of the sphere. Finally, geometries that are deemed too difficult to solve analytically, can be solved numerically, exemplified by the torus. A result of the project is a `Python` program that, when given one or more initial tangent circle pairs along the geodesic equations and metric tensor of a surface, constructs a geodesic circle packing using the described algorithm.

[1] `https://orbit.dtu.dk/en/persons/steen-markvorsen`
[2] `https://orbit.dtu.dk/en/persons/david-brander`

Contents

1 Introduction **3**

2 Methods and materials **3**
2.1 Generalization of the circle 3
2.2 Definition of a circle packing 4
2.3 A circle packing algorithm 5
2.4 Geodesics - straight lines on 2D surfaces 6
2.5 Solving the geodesic equation for selected surfaces 9
2.5.1 A plane 9
2.5.2 A cylinder 10
2.5.3 The Sphere 11
2.5.4 A torus 13
2.6 Numerical geodesic computations 14
2.7 Circle preserving maps 16

3 Experiments and results **19**
3.1 Packing with analytic solutions 19
3.2 Packing using numerical methods 25

4 Discussion **27**
4.1 Performance of algorithm 27
4.2 Analytic vs. numeric computations 27
4.3 Periodic domains 28
4.4 Using circles to visualize surfaces 28

5 Conclusion **30**

6 Outlook **31**

1 Introduction

How circles may be packed in the plane is a well known problem in geometry. There exist countless algorithms for doing so, with the common goal of fitting as many circles as possible within a given domain. A simple yet somewhat effective algorithm is one that constructs a packing by using tangent circle pairs to grow additional circles that can expand the packing. This algorithm is originally designed to pack circles in the plane, but it may be used to pack circles on surfaces living in 3D space as well.

The main focus of this project is to attempt generalizing the concept of a circle packing in the plane, to 2D surfaces living in 3D space. Naturally extending to figure out how one can use the tangent circle pair algorithm to pack circles on surfaces, and set up a computational framework for doing so.

The algorithm used will act as a stepping stone for implementation and testing of the developed theory, but the concepts may be applied to other algorithms as well, and it should therefore not be seen as the definitive answer as choice of algorithm to use in combination with the methods derived.

While there might be several practical applications of circle packings on surfaces, this report is exclusively concerned with the mathematical theory and task of making such packings, rather than investigating how they might be used in the real world.

2 Methods and materials

2.1 Generalization of the circle

In the plane $\mathbb{R}^2$, a circle is defined as the set of points a fixed euclidean distance r, denoted radius, from a fixed point c, known as the center. This definition allows for drawing circles in the plane, like the one in figure 1b, but restricts the concept of circles to exclusively exist in 2D euclidean spaces.

The notion of a circle can be generalized, by loosening the definition of radius to mean distance by any choice of metric, rather than euclidean distance. Thus different metrics of a 2D space can be chosen to obtain different looking circles. Figure 1 shows 3 examples of circles centered at $c = (0, 0)$ with radius $r = 1$, using different p-norms as the metric in the plane.

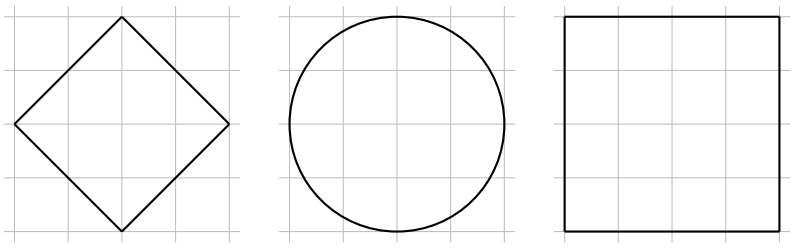

(a) 1-norm. (b) 2-norm. (c) ∞-norm

Figure 1: Visualization of circles in the plane for different metrics.

To clarify, in general metric spaces (M, d), circles with center c of radius r are defined as the set,

$$\{x \in M \mid d(x, c) = r\}. \tag{1}$$

In the terminology of metric spaces, these sets are often referred to as the boundary of an open ball $B_r(x)$[3].

It is important to emphasize that the concept of intersection generalizes as well. Consider two circles, C_1 and C_2, with radii and center r_1, c_1 and r_2, c_2 respectively. Analogue to the case of the euclidean plane, it is defined that C_1 and C_2 are intersecting if and only if the distance between their centers is less than or equal to their combined radius. Formally,

$$\text{Intersection condition: } d(c_1, c_2) \leq r_1 + r_2. \tag{2}$$

This also allows for generalization of the tangency concept, with C_1 and C_2 being tangent if and only if,

$$\text{Tangency condition: } d(c_1, c_2) = r_1 + r_2. \tag{3}$$

2.2 Definition of a circle packing

Following the definition of as, is a definition of what it means to pack circles within a domain.

The term "circle packing" refers to a set of non-overlapping circles within a given domain. The circles are allowed to touch each other, i.e being tangent. Having defined this, the immediate question of how such a packing may be constructed arises. This report is exclusively concerned with a specific algorithm that grows circles from tangent circle pairs, which is explained in detail by section 2.3.

[3] `https://en.wikipedia.org/wiki/Ball_(mathematics)`

2.3 A circle packing algorithm

Given two tangent circles in the plane, two new circles tangent to these may be constructed, namely one on either side of the tangent point as illustrated in figure 3. This creates 4 new tangent pairs from which additional circles can be grown. The circles should be grown as large as possible, which may be infinite size, if one does not impose some limitations.

To be classified as a circle packing algorithm, the growing of circles must satisfy the posed definition of a circle packing given in section 2.2. Thus circles should stop growing before leaving the domain or overlapping (referring to intersecting without being tangent) with circles already in the packing. Naturally, it may be desired to bound circle size from below, above or both. Collectively, this constitutes a set of rules that allows the algorithm to construct valid circle packings.

The algorithm terminates when no unchecked tangent circle pairs are left in the packing. For unbounded domains, this point may never be reached. The same holds true if there is no lower bound to the circle radius, as the space between a tangent pair and a new circle can hold more circles grown from the new tangent pairs, as illustrated in figure 2. Thus it is necessary to either define a lower bound on circle radius, or set a maximum for the allowed number of circles in the packing, and terminate when that is reached.

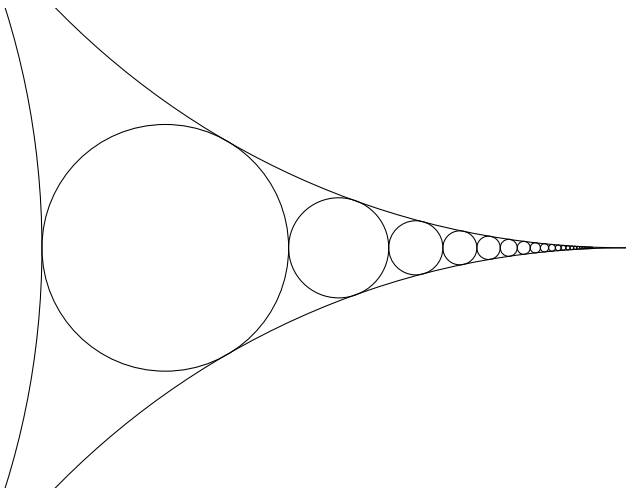

Figure 2: When circle size is not bounded from below the algorithm can run forever.

If the domain is bounded and circle size is bounded from below, the algorithm will always terminate. Suppose $\mathcal{D}$ is a domain with area $A_{\mathcal{D}}$ and the lower bound circle area is $A_{r_{\min}}$. The number of circles in any packing is then naturally upper bounded by $\frac{A_{\mathcal{D}}}{A_{r_{\min}}}$.

To run the algorithm, a growing curve $\gamma(t)$ must be determined. Consider

two tangent circles C_1 and C_2. Any new circle C_p on the grow curve with radius t and center $\gamma(t)$ must satisfy the tangency condition given in equation 3,

$$d(c_1, c_p) = r_1 + t, \quad d(c_2, c_p) = r_2 + t, \tag{4}$$

with r_1 and r_2 being the radii of C_1 and C_2 respectively. The grow curves, illustrated for the euclidean plane in figure 3, are thus obtained by solving system 4 for c_p.

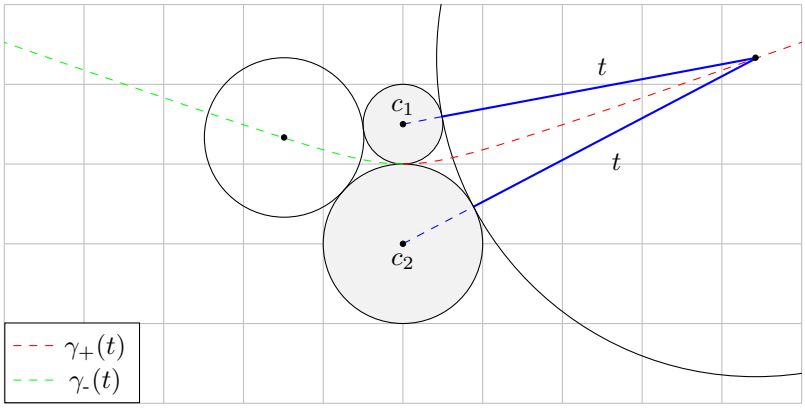

Figure 3: Visualization of circle packing algorithm.

2.4 Geodesics - straight lines on 2D surfaces

Having established a generalization of the circle concept, the problem of how one may choose a measure of distance arises. Naturally, it would be nice if the circles, when visualized in 3D space, appeared somewhat like euclidean circles in $\mathbb{R}^2$.

Euclidean circles, as mentioned, are defined through euclidean distance. A key property of this metric is that it measures the straight line distance between points in the plane (and all other euclidean spaces for the record). Straight line distance could hence be used on 2D surfaces as well. However, 2D surfaces are generally curved within 3D space, making what the definition of a straight line should be rather cryptic.

Two naive choices are to use either the euclidean distance in $\mathbb{R}^3$ as the metric for 2D surfaces in $\mathbb{R}^3$ or to use euclidean distance in the parameter domain of the surface. These choices might yield nice results on some surfaces, but does not work well in the general case. As an example, consider the parametrization of the unit sphere given by,

$$r(u, v) = [\cos(u)\sin(v), \sin(u)\sin(v), \cos(v)]^T, \quad u \in [0, 2\pi], \quad v \in [0, \pi].$$

Drawing an euclidean circle in the parameter domain of this sphere does not translate into something that resembles an euclidean circle. Figure 4 shows an example of this.

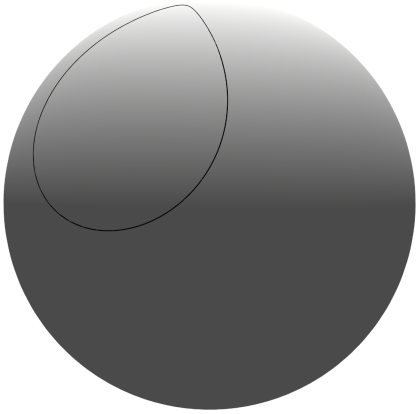

Figure 4: Circle of radius $\frac{\pi}{6}$ with center $\left(\pi, \frac{\pi}{4}\right)$ in the parameter domain of the unit sphere projected onto the unit sphere using parametrization 13.

What is needed, is a measure of straight line distance along the surface itself rather than its parameter domain or the space it lives in. This is quite obvious in the case of a plane, where a direct line between two points is considered straight. For general 2D surfaces it will in most cases not be possible to make such lines within the surface, thus another definition of straightness that may generalize the concept of straight paths is required.

A way to define a straight line, is a path that an object of constant speed follows when travelling along the surface. Put in other words, the object does not accelerate along the curve. This is the concept of geodesics curves. To clarify, geodesics generalize the concept of straight lines to 2D surfaces living in 3D space, by defining a straight line as a path of zero tangential acceleration.

Generally, a 2D surface can be represented by a parametrization, with parameters $(u^1, u^2) \in \Omega \subseteq \mathbb{R}^2$ and a vector function $\mathbf{r} : \Omega \to \mathbb{R}^3$. Similarly, a curve on that surface can also be represented by a parametrization $\mathbf{r}(\lambda(t))$ with $\lambda(t) = (u^1(t), u^2(t))$. As mentioned, in order for $\mathbf{r}(t)$ to be a geodesic, it must have zero tangential acceleration. The acceleration along the curve is given as its second order derivative, which may be computed by using the multivariate chain rule along the product rule. For the sake of compactness, Einstein summation notation[4] is used.

$$\frac{\partial^2 \mathbf{r}}{\partial t^2} = \frac{\partial^2 u^i}{\partial t^2} \frac{\partial \mathbf{r}}{\partial u^i} + \frac{\partial u^i}{\partial t} \frac{\partial}{\partial t} \frac{\partial \mathbf{r}}{\partial u^i}. \tag{5}$$

The first term is given by the first order derivatives of $\mathbf{r}$, thus already tangent to the surface. In the second term, it is not clear if it is tangent, normal or a combination of the two. First, the operator $\dfrac{\partial}{\partial t}$ is expanded as,

$$\frac{\partial}{\partial t} = \frac{\partial u^j}{\partial t} \frac{\partial}{\partial u^j}.$$

[4] https://en.wikipedia.org/wiki/Einstein_notation

Inserting into equation 5 then yields,

$$\frac{\partial^2 \mathbf{r}}{\partial t^2} = \frac{\partial^2 u^i}{\partial t^2}\frac{\partial \mathbf{r}}{\partial u^i} + \frac{\partial u^i}{\partial t}\frac{\partial u^j}{\partial t}\frac{\partial^2 \mathbf{r}}{\partial u^i u^j}. \tag{6}$$

As the second order partial derivatives are vectors living in 3D space, they may be expressed in terms of any valid basis. As the goal is to isolate tangential components of the acceleration, an appropriate choice of basis in this setting would be the two tangent vectors $\frac{\partial \mathbf{r}}{\partial u^1}$ and $\frac{\partial \mathbf{r}}{\partial u^2}$ given by the first order derivatives, along with a normal vector $\mathbf{n}$ that may be chosen as the normalized cross product of the tangent vectors. Thus,

$$\frac{\partial^2 \mathbf{r}}{\partial u^i u^j} = \Gamma^k_{ij}\frac{\partial \mathbf{r}}{\partial u^k} + L_{ij}\mathbf{n}, \quad \mathbf{n} = \frac{\frac{\partial \mathbf{r}}{\partial u^1} \times \frac{\partial \mathbf{r}}{\partial u^2}}{\left\| \frac{\partial \mathbf{r}}{\partial u^1} \times \frac{\partial \mathbf{r}}{\partial u^2} \right\|_2}, \tag{7}$$

Inserting into equation 6 and collecting terms of the basis vectors, one obtains,

$$\frac{\partial^2 \mathbf{r}}{\partial t^2} = \left(\frac{\partial^2 u^k}{\partial t^2} + \Gamma^k_{ij}\frac{\partial u^i}{\partial t}\frac{\partial u^j}{\partial t} \right)\frac{\partial \mathbf{r}}{\partial u^k} + L_{ij}\frac{\partial u^i}{\partial t}\frac{\partial u^j}{\partial t}\mathbf{n}. \tag{8}$$

Equation 8 provides the acceleration vector fully separated into a tangential part and a normal part. Recalling that geodesics have zero tangential acceleration, one arrive at the geodesic equation,

$$\frac{\partial^2 u^k}{\partial t^2} + \Gamma^k_{ij}\frac{\partial u^i}{\partial t}\frac{\partial u^j}{\partial t} = 0. \tag{9}$$

In order to determine Γ^k_{ij}, take the dot product on both sides of equation 7 with the tangent vector $\frac{\partial \mathbf{r}}{\partial u^l}$ to obtain,

$$\frac{\partial^2 \mathbf{r}}{\partial u^i u^j}\frac{\partial \mathbf{r}}{\partial u^l} = \left(\Gamma^k_{ij}\frac{\partial \mathbf{r}}{\partial u^k} + L_{ij}\mathbf{n} \right)\frac{\partial \mathbf{r}}{\partial u^l} = \Gamma^k_{ij}\frac{\partial \mathbf{r}}{\partial u^k}\frac{\partial \mathbf{r}}{\partial u^l},$$

as $\mathbf{n}$ by definition is orthogonal to $\frac{\partial \mathbf{r}}{\partial u^l}$. The quantities $\frac{\partial \mathbf{r}}{\partial u^k}\frac{\partial \mathbf{r}}{\partial u^l}$ are recognized as the components of the metric tensor G with components g_{kl}, thus,

$$\frac{\partial^2 \mathbf{r}}{\partial u^i u^j}\frac{\partial \mathbf{r}}{\partial u^l} = \Gamma^k_{ij} g_{kl}.$$

Applying the inverse metric tensor G^{-1}, with components g^{lm}, to the metric tensor yields the Kronecker delta[5], $g_{kl}g^{lm} = \delta_{km}$. Applying this gives,

$$\frac{\partial^2 \mathbf{r}}{\partial u^i u^j}\frac{\partial \mathbf{r}}{\partial u^l} g^{lm} = \Gamma^k_{ij}\delta_{km},$$

which by convention of the Kronecker delta simplifies to,

$$\Gamma^m_{ij} = \frac{\partial^2 \mathbf{r}}{\partial u^i u^j}\frac{\partial \mathbf{r}}{\partial u^l} g^{lm}, \tag{10}$$

[5] `https://en.wikipedia.org/wiki/Kronecker_delta`

with the metric tensor G given as,

$$G = \begin{bmatrix} \frac{\partial \mathbf{r}}{\partial u^1} \cdot \frac{\partial \mathbf{r}}{\partial u^1} & \frac{\partial \mathbf{r}}{\partial u^1} \cdot \frac{\partial \mathbf{r}}{\partial u^2} \\ \frac{\partial \mathbf{r}}{\partial u^1} \cdot \frac{\partial \mathbf{r}}{\partial u^2} & \frac{\partial \mathbf{r}}{\partial u^2} \cdot \frac{\partial \mathbf{r}}{\partial u^2} \end{bmatrix}. \tag{11}$$

Equation 10 is known as the Christoffel symbols of the surface, and having established these, geodesics can be found by solving the differential equation 9. Once the geodesics, $\lambda(t)$, have been obtained, the geodesic distance between two points is then obtained by the following integral giving the arc length,

$$L = \int_a^b \|\lambda'(t)\|_2 dt. \tag{12}$$

How geodesic circles look on 2D surfaces can be seen in the figures of section 3.

2.5 Solving the geodesic equation for selected surfaces

Having derived the required theoretical framework for determining geodesics on arbitrary 2D surfaces, this section is concerned with the computation of geodesics on some selected surfaces. Note that the variables (u^1, u^2) have been exchanged with (u, v) in an attempt to minimize confusion with powers and second order derivatives.

2.5.1 A plane

As geodesics are meant to generalize the concept of straight lines to any 2D surface, initially the base case of a plane is checked, before attempting 2D surfaces of higher complexity.

In a plane, geodesics are straight lines in the traditional sense, thus solving the geodesic equation 9 should result in exactly that.

Any plane living in 3D space can be parameterized by,

$$\mathbf{r}(u, v) = \mathbf{a}u + \mathbf{b}v + \mathbf{c} \quad u, v \in \mathbb{R},$$

with $\mathbf{a}$ and $\mathbf{b}$ being the basis vectors within the plane and $\mathbf{c}$ the translation of the plane from the origin. The first order partial derivatives are given as,

$$\frac{\partial \mathbf{r}(u, v)}{\partial u} = \mathbf{a}, \quad \frac{\partial \mathbf{r}(u, v)}{\partial v} = \mathbf{b},$$

followed by the second order partial derivatives,

$$\frac{\partial^2 \mathbf{r}(u, v)}{\partial u^2} = \frac{\partial^2 \mathbf{r}(u, v)}{\partial v^2} = \frac{\partial^2 \mathbf{r}(u, v)}{\partial u \partial v} = \frac{\partial^2 \mathbf{r}(u, v)}{\partial v \partial u} = \mathbf{0}.$$

It is seen that all Christoffel symbols (equation 10) are then 0. Thus the geodesic equation becomes,

$$\frac{\partial^2 u^k}{\partial t^2} = 0,$$

which is essentially 2 equations,

$$u''(t) = 0, \quad v''(t) = 0.$$

These are solved by integrating both sides twice to obtain,

$$u(t) = k_1 t + l_1, \quad v(t) = k_2 t + l_2.$$

Let $\mathbf{p}$ and $\mathbf{q}$ be two points within the plane. The boundary conditions $\lambda(0) = \mathbf{p}$ and $\lambda(1) = \mathbf{q}$ is then used to obtain a parametrization of the geodesic between $\mathbf{p}$ and $\mathbf{q}$ as,

$$\lambda(t) = (\mathbf{q} - \mathbf{p})t + \mathbf{p}.$$

The geodesic distance between $\mathbf{p}$ and $\mathbf{q}$ is then given by,

$$\int_0^1 \left\| \frac{\partial r(\lambda(t))}{\partial t} \right\|_2 dt = \sqrt{(p_1 - q_1)^2 + (p_2 - q_2)^2},$$

which is the euclidean distance between them, as expected.

2.5.2 A cylinder

Having verified the case of the plane, the cylinder is examined next. A cylinder is characterized by a radius R and a height H. Without loss of generality, assume that the bottom of the cylinder is centered at the origin of the (x, y) plane at $z = 0$. If not, one may rotate and translate the cylinder to obtain such a positioning. In this setting, the cylinder may be parameterized by,

$$\mathbf{r}(u, v) = \begin{bmatrix} R\cos(u) \\ R\sin(u) \\ v \end{bmatrix}, \quad u \in [0, 2\pi], \quad v \in [0, H].$$

The first order partial derivatives are given as,

$$\frac{\partial \mathbf{r}(u, v)}{\partial u} = \begin{bmatrix} -R\sin(u) \\ R\cos(u) \\ 0 \end{bmatrix}, \quad \frac{\partial \mathbf{r}(u, v)}{\partial v} = \begin{bmatrix} 0 \\ 0 \\ 1 \end{bmatrix},$$

followed by the second order partial derivatives,

$$\frac{\partial^2 \mathbf{r}(u, v)}{\partial u^2} = \begin{bmatrix} -R\cos(u) \\ -R\sin(u) \\ 0 \end{bmatrix}, \quad \frac{\partial^2 \mathbf{r}(u, v)}{\partial v^2} = \frac{\partial^2 \mathbf{r}(u, v)}{\partial u \partial v} = \frac{\partial^2 \mathbf{r}(u, v)}{\partial v \partial u} = \mathbf{0}.$$

As there in this case are non-zero second order partial derivatives, one must compute the Christoffel symbols. Starting by computing the metric tensor and its inverse as,

$$G = \begin{bmatrix} R^2 & 0 \\ 0 & 1 \end{bmatrix}, \quad G^{-1} = \begin{bmatrix} \frac{1}{R^2} & 0 \\ 0 & 1 \end{bmatrix}.$$

As the second order derivative with respect to u is the only non-zero second order partial derivative, it is certain that all Christoffel symbols that are not Γ^1_{11} and Γ^2_{11} are 0. Examining the last 2 Christoffel symbols yields,

$$\Gamma^1_{11} = \frac{1}{R^2}\begin{bmatrix} -R\sin(u) \\ R\cos(u) \\ 0 \end{bmatrix} \cdot \begin{bmatrix} -R\cos(u) \\ -R\sin(u) \\ 0 \end{bmatrix} = 0,$$

$$\Gamma^2_{11} = \begin{bmatrix} -R\sin(u) \\ R\cos(u) \\ 0 \end{bmatrix} \cdot \begin{bmatrix} 0 \\ 0 \\ 1 \end{bmatrix} = 0.$$

In conclusion, all Christoffel symbols are 0, thus the geodesic equation is equivalent to that of the plane. This can be attributed to the fact that the cylinder is essentially a rolled up plane. The solution is thus given as,

$$\lambda(t) = (\mathbf{q} - \mathbf{p})t + \mathbf{p}.$$

with $\mathbf{p}$ and $\mathbf{q}$ being points on the cylinder. Such a curve on the surface of a cylinder is known as a helix. The distance between $\mathbf{p}$ and $\mathbf{q}$ is then given by,

$$\int_0^1 \left| \frac{\partial r(\lambda(t))}{\partial t} \right|_2 dt = \sqrt{R^2(p_1 - q_1)^2 + (p_2 - q_2)^2}.$$

As the cylinder allows one to go all the way around, this distance may not be the shortest. In fact, if $|p_1 - q_1| > \pi$, the shortest path is to go the other way around the cylinder. As $p_1 - q_1$ essentially measures angular difference of the 2 points, it may be replaced by the accurate formula obtained through angle between vectors,

$$\Delta u = \arccos(\cos(p_1)\cos(q_1) + \sin(p_1)\sin(q_1)),$$

thus the geodesic distance is given by,

$$d(p, q) = \sqrt{R^2(\Delta u)^2 + (p_2 - q_2)^2}.$$

This goes to show that the geometry of some surfaces allow for several geodesics between 2 points. However, the geodesic distance is defined as the length of the shortest geodesic between the points.

2.5.3 The Sphere

The sphere is defined as the set of points a fixed euclidean distance from a center point. As the geometry of a sphere is the same regardless of radius and placement within 3D space, it can be assumed that the sphere is centered at the origin and has radius 1. If not, it may be translated and scaled to be so. The unit sphere can be parameterized as,

$$\mathbf{r}(u, v) = \begin{bmatrix} \cos(u)\sin(v) \\ \sin(u)\sin(v) \\ \cos(v) \end{bmatrix}, \quad u \in [0, 2\pi], \quad v \in [0, \pi]. \tag{13}$$

The first order partial derivatives are given as,

$$\frac{\partial \mathbf{r}(u,v)}{\partial u} = \begin{bmatrix} -\sin(u)\sin(v) \\ \cos(u)\sin(v) \\ 0 \end{bmatrix}, \quad \frac{\partial \mathbf{r}(u,v)}{\partial v} = \begin{bmatrix} \cos(u)\cos(v) \\ \sin(u)\cos(v) \\ -\sin(v) \end{bmatrix},$$

followed by the second order partial derivatives,

$$\frac{\partial^2 \mathbf{r}(u,v)}{\partial u^2} = \begin{bmatrix} -\cos(u)\sin(v) \\ -\sin(u)\sin(v) \\ 0 \end{bmatrix}, \quad \frac{\partial^2 \mathbf{r}(u,v)}{\partial v^2} = \begin{bmatrix} -\cos(u)\sin(v) \\ -\sin(u)\sin(v) \\ -\cos(v) \end{bmatrix},$$

$$\frac{\partial^2 \mathbf{r}(u,v)}{\partial u \partial v} = \frac{\partial^2 \mathbf{r}(u,v)}{\partial v \partial u} = \begin{bmatrix} -\sin(u)\cos(v) \\ \cos(u)\cos(v) \\ 0 \end{bmatrix}.$$

Next the metric tensor and its inverse are computed as,

$$G = \begin{bmatrix} \sin^2(v) & 0 \\ 0 & 1 \end{bmatrix}, \quad G^{-1} = \begin{bmatrix} \sin^{-2}(v) & 0 \\ 0 & 1 \end{bmatrix}.$$

This allows for the usage of formula 10 to compute the Christoffel symbols,

$$\Gamma^1 = \begin{bmatrix} 0 & \cot(v) \\ \cot(v) & 0 \end{bmatrix}, \quad \Gamma^2 = \begin{bmatrix} 0 & 0 \\ 0 & -\cos(v)\sin(v) \end{bmatrix}.$$

Inserting into the geodesic equation gives the following system,

$$u''(t) + 2\cot(v(t))v'(t)u'(t) = 0 \tag{14}$$

$$v''(t) - \cos(v(t))\sin(v(t))u'(t)^2 = 0 \tag{15}$$

This is a coupled system of non-linear differential equations, which are generally difficult to solve. While it is indeed possible to solve these equations analytically, it is quite comprehensive. Instead of explicitly solving the equations, one may consider the nature and symmetry of the sphere to make a guess on the geodesics and check if it satisfies the geodesic equation. An educated guess would be that of a great circle, as it seems reasonable that moving forwards without turning on a sphere results in such a path.

As the sphere is symmetric around any axis through its center, it suffices to check a single great circle of the sphere. A simple choice would be the equator. While at it, one may as well check all latitude paths. For a fixed latitude v_0, the path around the sphere is given as,

$$\lambda(t) = \begin{bmatrix} u(t) \\ v(t) \end{bmatrix} = \begin{bmatrix} t \\ v_0 \end{bmatrix},$$

with first and second order derivatives,

$$u'(t) = 1, \quad u''(t) = v'(t) = v''(t) = 0.$$

Inserting into (14) gives,

$$0 + 2\cot(0) \cdot 0 \cdot 0 = 0,$$

which is always satisfied. Inserting into (15) gives,

$$0 - \cos(v_0)\sin(v_0)\,1^2 = 0,$$

implying that $\cos(v_0)\sin(v_0) = 0$. Within the domain of v, which is $[0, \pi]$, there are 3 possible solutions. 0 and π results in the north and south pole respectively, which are stationary points and thus not that interesting. The last solution is $\frac{\pi}{2}$ which is a great circle path around the equator. This shows that great circles are the only circles that are geodesics on the sphere. On a side note, it is possible to show that great circles are indeed the only geodesics on the sphere, but this is not done in this report as mentioned earlier.

The distance between 2 points $\mathbf{p}$ and $\mathbf{q}$ on a great circle can then be computed as the angle between vectors in 3D space.

$$d(\mathbf{p}, \mathbf{q}) = R\ \arccos(\mathbf{p} \cdot \mathbf{q}),$$

with R being the radius of the sphere in the general case.

2.5.4 A torus

The final surface that is explicitly derived is the torus. Unlike the cylinder and the sphere, a torus has both positive and negative curvature, which generally makes for a more complicated surface. A torus is characterized by 2 radii, R_1 denoting the radius of the circle in the center of the torus and R_2 denoting the radius of the ring itself. Assumed centered at the origin, it is parameterized by,

$$\mathbf{r}(u, v) = \begin{bmatrix} (R_1 + R_2\cos(v))\cos(u) \\ (R_1 + R_2\cos(v))\sin(u) \\ R_2\sin(v) \end{bmatrix}, \quad u \in [0, 2\pi], \quad v \in [0, 2\pi]. \tag{16}$$

The first order partial derivatives are given as,

$$\frac{\partial \mathbf{r}(u,v)}{\partial u} = \begin{bmatrix} -(R_1 + R_2\cos(v))\sin(u) \\ (R_1 + R_2\cos(v))\cos(u) \\ 0 \end{bmatrix}, \quad \frac{\partial \mathbf{r}(u,v)}{\partial v} = \begin{bmatrix} -R_2\sin(v)\cos(u) \\ -R_2\sin(v)\sin(u) \\ R_2\cos(v) \end{bmatrix},$$

followed by the second order partial derivatives,

$$\frac{\partial^2 \mathbf{r}(u,v)}{\partial u^2} = \begin{bmatrix} -(R_1 + R_2\cos(v))\cos(u) \\ -(R_1 + R_2\cos(v))\sin(u) \\ 0 \end{bmatrix}, \quad \frac{\partial^2 \mathbf{r}(u,v)}{\partial v^2} = \begin{bmatrix} -R_2\cos(v)\cos(u) \\ -R_2\cos(v)\sin(u) \\ -R_2\sin(v) \end{bmatrix},$$

$$\frac{\partial^2 \mathbf{r}(u,v)}{\partial u \partial v} = \frac{\partial^2 \mathbf{r}(u,v)}{\partial v \partial u} = \begin{bmatrix} R_2\sin(v)\sin(u) \\ -R_2\sin(v))\cos(u) \\ 0 \end{bmatrix}.$$

Next the metric tensor and its inverse are computed as,

$$G = \begin{bmatrix} (R_1 + R_2\cos(v))^2 & 0 \\ 0 & R_2^2 \end{bmatrix}, \quad G^{-1} = \begin{bmatrix} (R_1 + R_2\cos(v))^{-2} & 0 \\ 0 & R_2^{-2} \end{bmatrix}.$$

This allows for the usage of formula 10 to compute the Christoffel symbols,

$$\Gamma^1 = \begin{bmatrix} 0 & -\frac{R_2 \sin(v)}{R_1 + R_2 \cos(v)} \\ -\frac{R_2 \sin(v)}{R_1 + R_2 \cos(v)} & 0 \end{bmatrix}, \quad \Gamma^2 = \begin{bmatrix} \frac{(R_1 + R_2 \cos(v)) \sin(v)}{R_2} & 0 \\ 0 & 0 \end{bmatrix}.$$

Inserting into the geodesic equation then gives the following system,

$$u''(t) - \frac{2R_2 \sin(v(t))}{R_1 + R_2 \cos(v(t))} v'(t) u'(t) = 0 \tag{17}$$

$$v''(t) + \frac{(R_1 + R_2 \cos(v(t))) \sin(v(t))}{R_2} u'(t)^2 = 0, \tag{18}$$

which is a coupled system of non-linear ordinary differential equations. This system is very difficult to solve, and does not generally have a nice closed form solution. It is however possible to derive some geodesics of the torus. It is seen that the equations are satisfied if $u(t)$ is constant and $v(t)$ is linear, resulting in vertical circles around the torus. They are also satisfied by $u(t)$ being linear and $v(t)$ equalling a multiple of π, resulting in the inner and outer horizontal rings of the torus. These are rather simple geodesics and obtaining further solutions analytically, is quite difficult. Alternatively, numerical methods can be used instead as explained in detail in section 2.6. The geodesics that have just been described are visualized as the black curves in figure 5, along another geodesic showed in blue that is computed numerically.

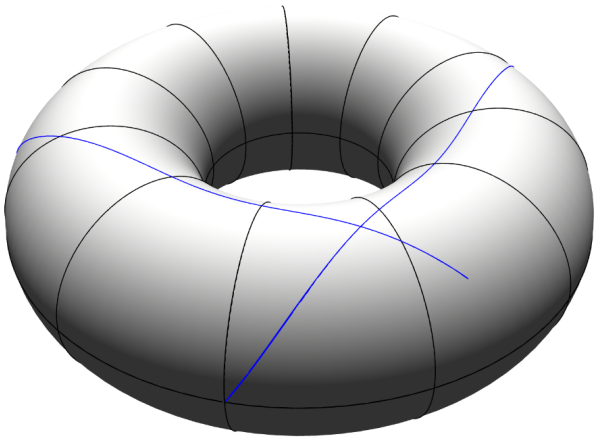

Figure 5: Geodesics of a torus with $R_1 = 1$, $R_2 = 0.5$.

2.6 Numerical geodesic computations

The general case of the geodesic equation is difficult to solve analytically. This section provides a numerical method of using the geodesic equation to approximate geodesics as well as geodesic circles.

The general case of the geodesic equation for 2D surfaces, is essentially a

coupled system of ordinary second order non-linear differential equations.

$$\frac{\partial^2 u^1}{\partial t^2} = -\Gamma^1_{ij}\frac{\partial u^i}{\partial t}\frac{\partial u^j}{\partial t}$$
$$\frac{\partial^2 u^2}{\partial t^2} = -\Gamma^2_{ij}\frac{\partial u^i}{\partial t}\frac{\partial u^j}{\partial t}$$

By defining $w^1(t) = (u^1(t))'$ and $w^2(t) = (u^2(t))'$, the system reduces to the following first order system,

$$\begin{aligned}(u^1(t))' &= w^1(t)\\ (u^2(t))' &= w^2(t)\\ (w^1(t))' &= -\Gamma^1_{ij}(u^i(t))'(u^j(t))'\\ (w^2(t))' &= -\Gamma^2_{ij}(u^i(t))'(u^j(t))'.\end{aligned}$$

Given an initial position $\mathbf{p}$ and a velocity vector $\mathbf{v}$, methods such as Runge Kutta[6] can be used to approximate geodesic curves. The geodesic distance between points may be obtained through use of a shooting method[7].

A geodesic circle centered at $\mathbf{p}$ of radius r can be approximated by shooting a length of r in N uniform directions on the interval $[0, 2\pi]$. By the geodesic equation, the tangential acceleration is 0, implying the speed is constant. Thus choosing an initial velocity of magnitude 1 on the surface and shoot r units will result in a geodesic curve of length r from $\mathbf{p}$. The velocity $\mathbf{v}$ is normalized through use of the first fundamental form of the surface according to equation 19,

$$e_{\mathbf{v}} = \frac{\mathbf{v}}{\sqrt{\mathbf{v}^T G(\mathbf{p})\mathbf{v}}}, \tag{19}$$

with G being the metric tensor of the surface. Figure 6 shows a visual representation of the method for approximating geodesic circles, using a coarse approximation for visualization purposes.

[6] https://en.wikipedia.org/wiki/Runge%E2%80%93Kutta_methods
[7] https://en.wikipedia.org/wiki/Shooting_method

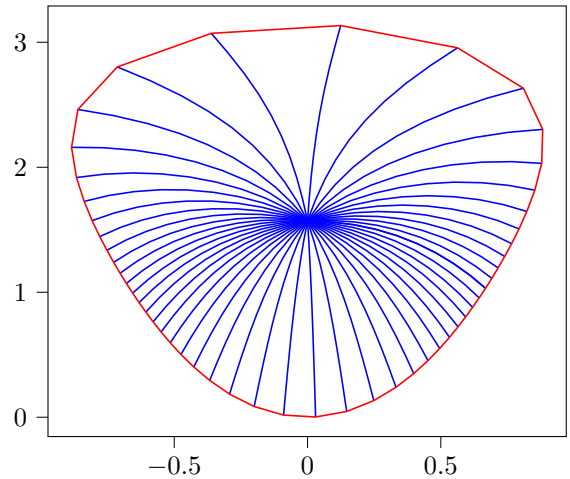

Figure 6: Approximation of geodesic circle with center $(0, \frac{\pi}{2})$ and radius $\frac{\pi}{4}$ on a torus defined by $R_1 = 1$ and $R_2 = \frac{1}{2}$. $N = 50$.

2.7 Circle preserving maps

As it has been seen, the general case of finding geodesics is often quite difficult. A suggestion to simplify the task of packing geodesic circles, is to construct a parametrization such that euclidean circles in the parameter domain maps to geodesic circles on the surface. Such a parametrization simplifies the problem to a task of packing circles in $\mathbb{R}^2$.

There exists several examples of such parametrizations, of which some will be tested later in the report. An example for the sphere will now be explained in detail.

The stereographic projection uses the entire plane as the parameter domain for a parametrization of the sphere. Considering the unit sphere S^2, the stereographic projection and its inverse is given by,

$$f : S^2 \to \mathbb{R}^2,$$

$$f(x, y, z) = \left[\frac{x}{1-z}, \frac{y}{1-z}\right], \tag{20}$$

$$f^{-1}(X, Y) = \left[\frac{2X}{1+X^2+Y^2}, \frac{2Y}{1+X^2+Y^2}, \frac{-1+X^2+Y^2}{1+X^2+Y^2}\right]. \tag{21}$$

In section 2.5.3 it is shown that geodesics on a sphere are given by great circles, and thus the geodesic distance between 2 points on a sphere is given by the great circle distance. Combined with the symmetry of the sphere, it is seen that geodesic circles on a sphere are circles in $\mathbb{R}^3$ defined by the intersection of a plane with the sphere.

Proceeding to show that the stereographic projection preserves circles, and

thus maps circles in the plane to geodesic circles on the sphere. Consider the definitions of circles in the plane and on the sphere respectively. In $\mathbb{R}^2$, a circle is a set of points (X, Y) that satisfy equation 22 for some $a, b, R \in \mathbb{R}$.

$$(X - a)^2 + (Y - b)^2 = R^2. \tag{22}$$

A circle on the surface of the unit sphere may be described as the intersection between the sphere and a plane in $\mathbb{R}^3$. Formally, it is the set of points that satisfies equations 23 and 24 for some $a, b, c, d \in \mathbb{R}$, i.e are both on the sphere and in the plane.

$$x^2 + y^2 + z^2 = 1, \tag{23}$$
$$ax + by + cz = d. \tag{24}$$

Generally, one can define the plane using a unit normal vector $n = [n_1, n_2, n_3]$ and a shift of d units in its direction. For the case of the unit sphere, that means,

$$n_1 x + n_2 y + n_3 z = d.$$

Note that the plane is tangent to S^2 if $|d| = 1$, with a single point of intersection rather than a circle. For $|d| > 1$ the plane does not intersect S^2 at all. Thus circles of intersection between the plane and S^2 only exist when $|d| < 1$. Formally, a circle $C \in S^2$ is defined as,

$$C = \{(x, y, z) \in S^2 \mid n_1 x + n_2 y + n_3 z = d,\ ||n|| = 1,\ |d| < 1\}.$$

Substituting (x, y, z) using the inverse stereographic projection f^{-1} (21), one gets,

$$n_1 \frac{2X}{1 + X^2 + Y^2} + n_2 \frac{2Y}{1 + X^2 + Y^2} + n_3 \frac{-1 + X^2 + Y^2}{1 + X^2 + Y^2} = d.$$

Which can be rearranged as,

$$(n_3 - d)X^2 + 2n_1 X + (n_3 - d)Y^2 + 2n_2 Y = n_3 + d.$$

If $n_3 = d$, one gets the straight line,

$$n_1 X + n_2 Y = d.$$

In this case, the north pole of S^2 given by $(0, 0, 1)$ is part of the circle on the unit sphere. This point is said to be projected at $\pm\infty$, hence in some sense a circle of infinite radius. Proceeding by assuming $n_3 \neq d$, one may divide by $n_3 - d$ and complete squares to obtain,

$$\left(X + \frac{n_1}{n_3 - d}\right)^2 + \left(Y + \frac{n_2}{n_3 - d}\right)^2 = \frac{1 - d^2}{(n_3 - d)^2},$$

which is the equation of a circle in $\mathbb{R}^2$, thus showing that the inverse stereographic projection does preserve circles. Note that the case where circles are projected onto straight lines, is irrelevant when using the inverse projection in the context of mapping the plane to the sphere. However, it does pose a natural restriction upon the packings one can make, as circles cannot contain the north pole itself but only get arbitrarily close. A workaround is to initially make a

circle containing the north pole, and use the projection of that circle onto the plane as a boundary for the packing.

While the stereographic projection does preserve circles, it does not preserve size. Distances gets increasingly stretched longer as the north pole is approached. Therefore, it is necessary to have control of the size of circles on the sphere when defining them in the plane. Put in other terms, how circle sizes on the sphere gets distorted in the plane.

Due to the rotational symmetry of this problem, the relation between radii on the sphere and in the plane through the stereographic projection may be derived in one dimension, namely a slice through the origin as illustrated in figure 7.

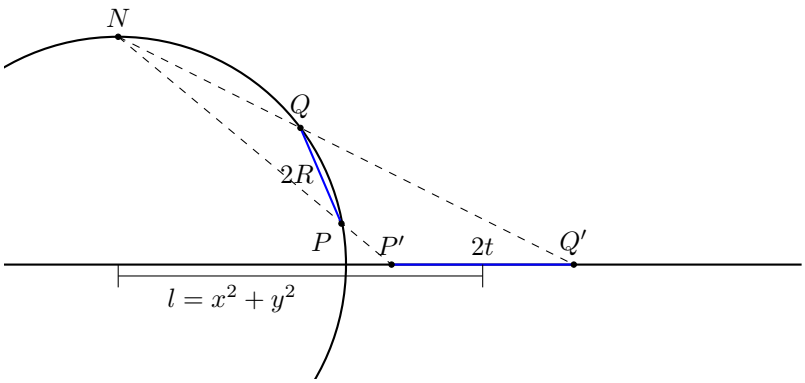

Figure 7: Trigonometric relation between circles on the sphere and $\mathbb{R}^2$.

Let l be the distance from the origin to the center of a circle in the plane, and t its radius. The points $l \pm t$ are antipodals on the circle. The half distance between the corresponding two points on S^2 is then the radius of the circle on the sphere. Formally, when the circle in the plane with center (x, y) and radii t is projected onto the sphere, it has radii,

$$\begin{aligned} R &= \frac{1}{2}\sqrt{\left(\frac{2(l+t)}{1+(l+t)^2} - \frac{2(l-t)}{1+(l-t)^2)}\right)^2 + \left(\frac{(l+t)^2-1}{1+(l+t)^2} - \frac{(l-t)^2-1}{1+(l-t)^2}\right)^2} \\ &= \sqrt{\frac{4t^2}{t^4+(1-l^2)2t^2+(l^2+1)^2}} \\ &= \sqrt{\frac{4t^2}{t^4+(1-x^2-y^2)2t^2+(x^2+y^2+1)^2}} \end{aligned} \tag{25}$$

As t increases, the radii on the sphere will eventually decrease due to the higher order term in the denominator of equation 25. This is due to the circle exceeding the equator of the sphere and thus shrinking towards the north pole. Another

observation is that this can only happen if the origin is contained within the circle in the plane as the north pole is unreachable. One may simplify the problem and avoid this by having the initial circles containing the origin.

As mentioned, the boundary of the packing should be a circle containing the north pole. The radius of such a boundary circle may computed by letting $x = y = 0$ in equation 25 and solve for R. Doing so provides 2 positive real solutions for the radius, as there exist two circles in the plane mapped to circles of equal radii on the sphere, one on either side. The desired circle is the one on the upper hemisphere, which have radius,

$$t = \frac{1 + \sqrt{-R^2 + 1}}{R}. \tag{26}$$

Naturally, equation 26 shows that R can be at most 1 and tiny values of R results in large values of t.

When performing the circle packing algorithm to pack on the sphere through the stereographic projection, the bounds on circle size are only fixed on the sphere, and thus dynamic according to equation 25 in the plane, with x and y as functions of t according to the circle growing curves defined in equation 4. When getting close to the north pole, equation 25 may not be solvable for the desired radii, as even circles of infinite size may never be large enough. This is solved by setting the upper bound on circle size as the limit of equation 25 as $t \to \infty$.

3 Experiments and results

3.1 Packing with analytic solutions

The simplest case of the algorithm given in section 2.3, is that of the plane. As shown in section 2.5, geodesics of the plane are straight lines with ordinary circles as geodesic circles. The grow curves are obtained by solving system 4 using euclidean distance as d, resulting in the grow curve $\gamma(t)$,

$$\gamma(t) = \begin{bmatrix} x(t) \\ y(t) \end{bmatrix}, \quad x(t) = \pm \frac{2\sqrt{r_1 r_2 (r_1 + r_2 + t)\, t}}{r_1 + r_2}, \quad y(t) = \frac{r_1 - r_2}{r_1 + r_2}\, t, \quad t > 0.$$

The $\pm$ on $x(t)$ represents the 2 circles one may grow.

To test the numerical accuracy of the implementation of the algorithm, the first packing is made using a fixed circle size and a rectangular domain. With only one circle size, the expected output would be a hexagonal pattern. Making such a packing could potentially fail, if the implementation is somehow unable to detect tangent pairs. Figure 8 shows that the implementation does indeed make a packing with hexagonal patterns, thus tangent pairs are indeed detected.

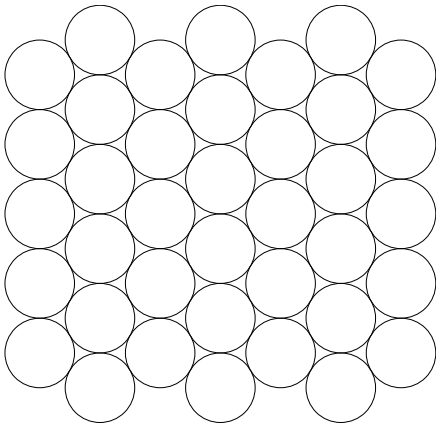

Figure 8: Running algorithm with fixed a circle size of $r = 0.15$ within a 2 by 2 rectangle.

A natural follow up is to set a range for circle size, giving the algorithm more freedom. Figure 8 shows a packing in which circle radii can vary by a factor of up to 15. Thus the implementation is capable of handling a range of circle sizes to make the packing. One may also try other domains such as a circle which is shown in figure 10.

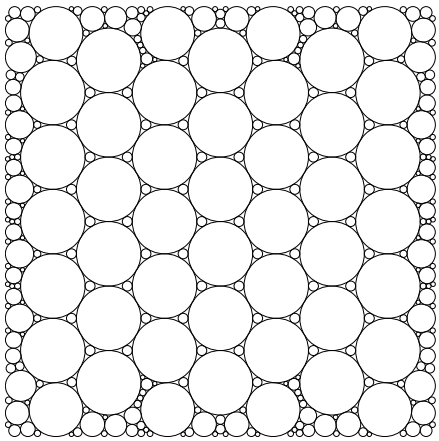

Figure 9: Running algorithm with circle size range $r \in [0.01, 0.15]$ within a 2 by 2 rectangle.

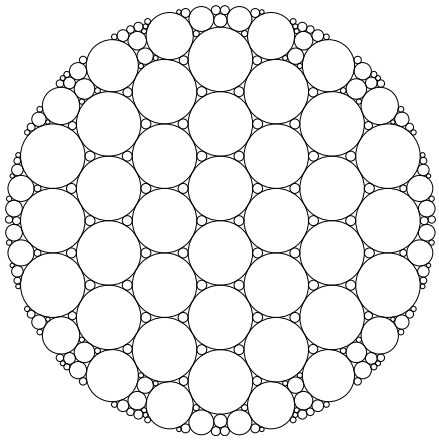

Figure 10: Running algorithm with circle size range $r \in [0.01, 0.15]$ within the unit circle.

Common for the domains is that the algorithm seems to pack as many circles of the largest radius as possible, and then fill in the gaps with smaller circles. It does make sense recalling that circles are grown to the largest size possible and nothing is in the way to prevent them from doing so. To see what happens if the algorithm encounters obstacles, a run has been made where a large circle has been placed inappropriately in an attempt to break the pattern. The resulting packing is shown in figure 11, in which it is seen that the large hexagonal pattern is no longer present.

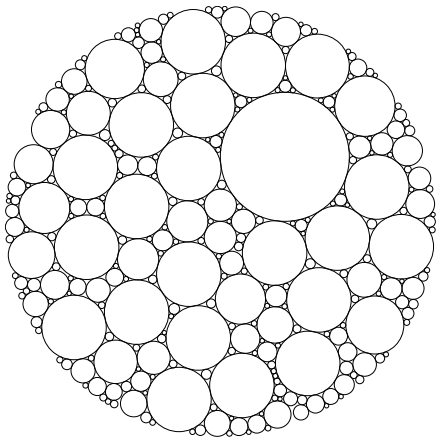

Figure 11: Running algorithm with circle size range $r \in [0.01, 0.15]$ within the unit circle, a large circle of radius 0.3 is placed as an obstacle before running the algorithm.

To make the implementation as versatile as possible, it has been equipped with the capability of packing circles within a domain specified by a binary

image. In the binary image, 0 represents the domain whereas 1 represents obstacles. Naturally the border of the image is a boundary of the domain as well. This functionality is demonstrated in figure 12, and can also be seen on the front page of this report.

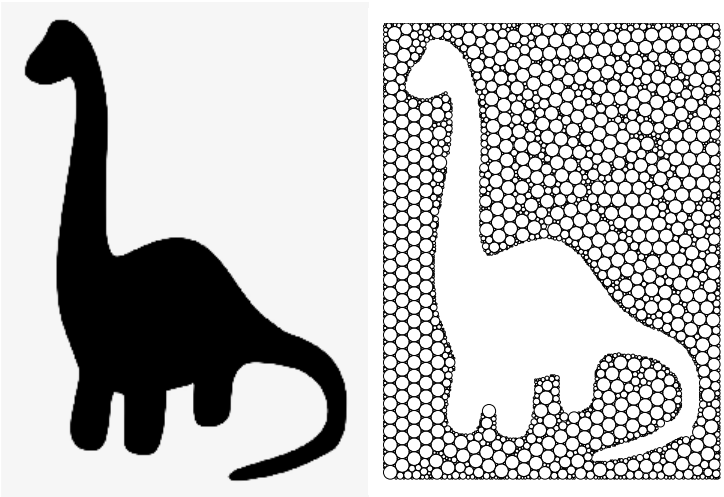

Figure 12: Constructing a circle packing in a domain given by a binary image of a dinosaur.

In the upper right part of figure 12, it is noticed that there seems to be pieces of hexagonal patterns. It is like shards of hexagonal patterns held together by smaller circles.

As discovered in section 2.5, the cylindrical map from the plane to a cylinder maps circles onto geodesics. Therefore, the implementation from the plane can be reused on the cylinder, with the slight modification of the u parameter being periodic. A circle packing of the parameter domain of a cylinder is presented in figure 13, and visualized on the surface of the cylinder in figure 14. The implementation packs tight along the top and bottom border of the domain, but make patterns that fit together along the sides.

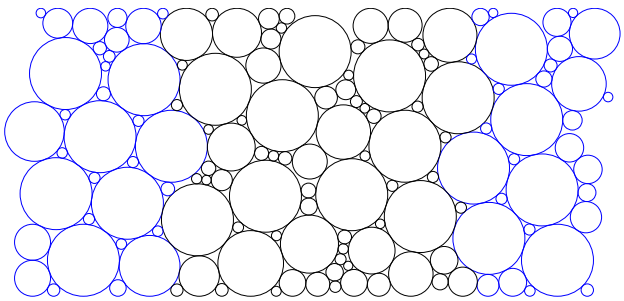

Figure 13: Circle packing in the domain of a cylinder. Horizontal axis is periodic as shown by the blue regions.

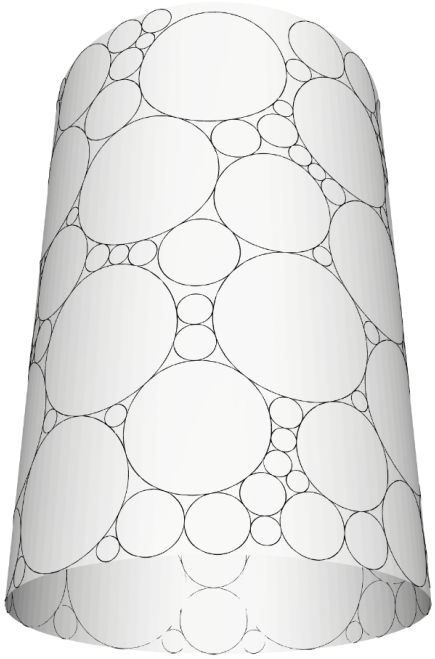

Figure 14: Circle packing in figure 13 visualized on the surface of the cylinder.

The final packing done analytically, is the surface of the unit sphere through use of the stereographic projection described in section 2.7. The visuals of the packing in the parameter domain is slightly different to that of the plane and cylinder, as circles must get larger when get further from the origin in order to maintain the range for the radius on the sphere. This is seen in left part of figure 15, where the circles seem to grow rapidly in size but are in fact all the same size as seen in the right part of figure 15. The algorithm is also run for variable circles sizes in figure 16, which is seen to form a somewhat tight packing with few gaps.

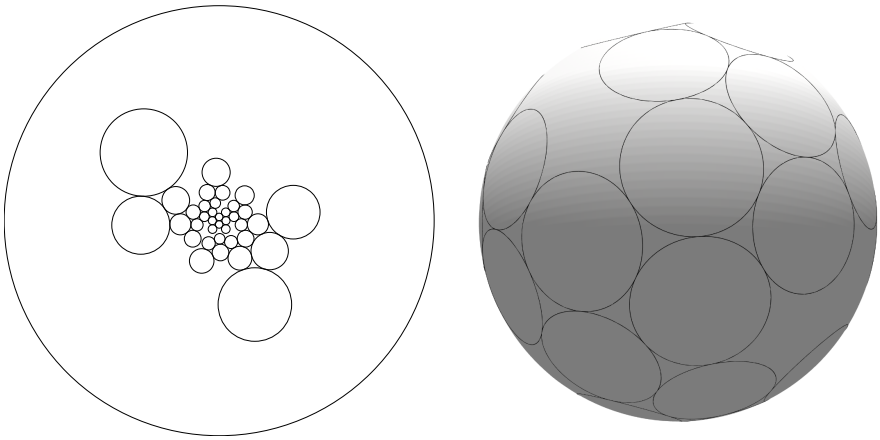

Figure 15: Circle packing of the unit sphere with fixed circle radius using the stereographic projection.

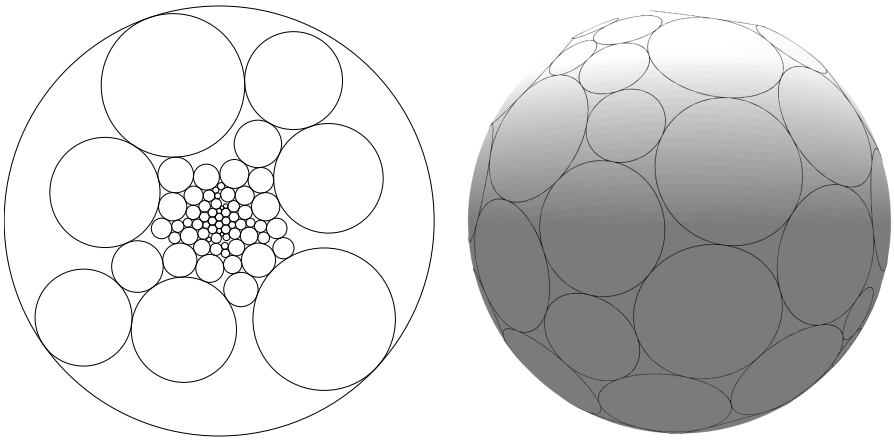

Figure 16: Circle packing of the unit sphere with variable circle radius using the stereographic projection.

There are large gaps in the packing of figure 15, where the circles size is fixed, unlike the plane in which tight hexagonal patterns form. To see emphasize this, figure 17 has been made. Here it can be seen that a lot of space is left unpacked. The circle size used in figure 17 is quite small, hence hexagonal formations of 7 circles occasionally form most likely due to numerical instabilities in the implementation. These formations are theoretically not possible on the sphere in this setting.

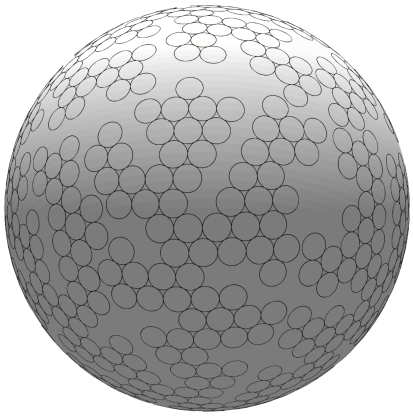

Figure 17: Circle packing of the unit sphere with fixed circle radius using the stereographic projection.

3.2 Packing using numerical methods

In order to pack geodesic circles on surfaces deemed too difficult to solve analytically, a numeric solver has been implemented to perform the task instead. The implementation has been tested on 3 surfaces. The first surface is the sphere, chosen in order to compare results with the analytic packing on the sphere. The second surface is that given by a quadratic function to show appliance to surfaces given by multivariate functions. The third surface is the torus as the complexity of its geometry makes it very difficult to solve analytically.

Circles in the parameter domains of these surfaces are generally not mapped to geodesic circles on the surfaces themselves. This can be seen in both figure 18 and 20.

Figure 18 shows that the numerical solver does create a packing on the sphere similar to that made by the analytical implementation, indicating that the numerical solver does indeed work as a tool for constructing geodesic circle packings.

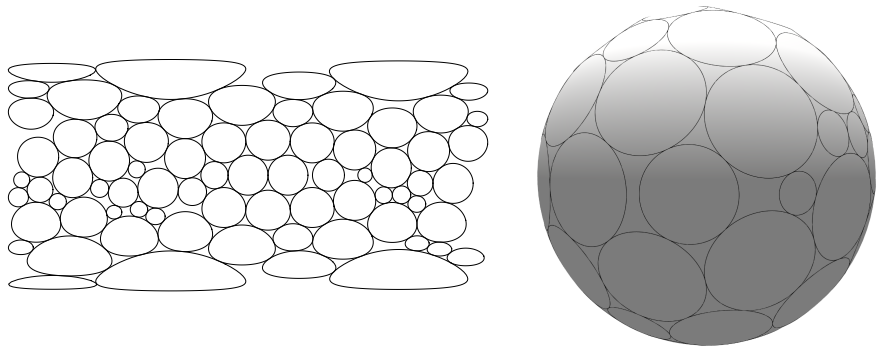

Figure 18: Circle packing of the unit sphere, given by the parametrization 13, with variable circle radius using numerical solver.

Figure 19 shows a circle packing on a quadratic surface. Worth noting is that some of the corners of the domain are not packed. This is not due to lack of space, as can be seen in the 3D visualization, but is rather a consequence of how the algorithm works. Notice that there are no tangent pairs from which circles can be grown to fill the blank areas.

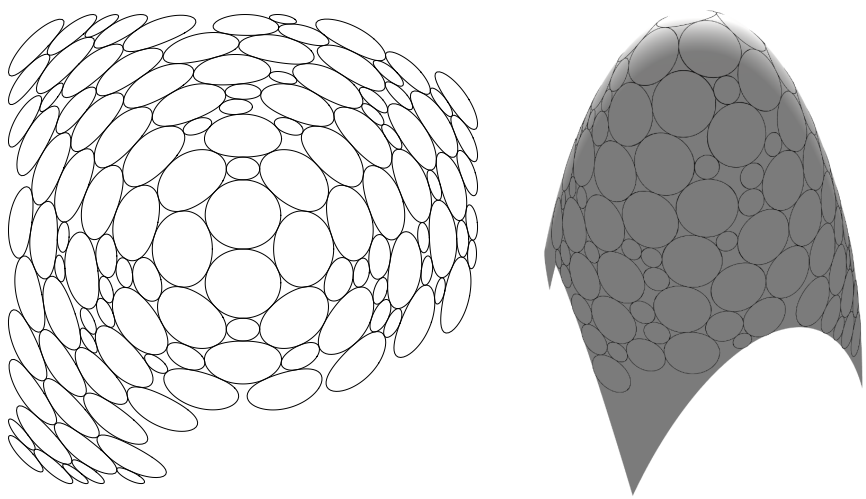

Figure 19: Circle packing on the quadratic surface given by $f(u, v) = -u^2 - v^2$ using numerical solver.

Finally, the method is tested to make a packing on the torus. Figure 20 show the results of running the algorithm. It is seen that it does indeed make a nice somewhat tight packing of geodesic circles.

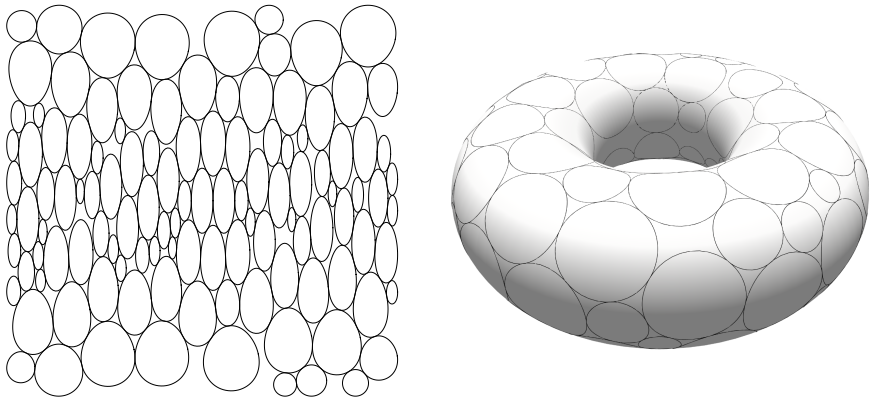

Figure 20: Circle packing of a torus, using parametrization 16 $R_1 = 1$ and $R_2 = 0.5$, with variable circle radius using numerical solver.

4 Discussion

4.1 Performance of algorithm

As all packings in this report are made using the same algorithm, it is appropriate to address some of its issues. Generally, it makes nice and somewhat tight packings in the plane. It can naturally only form pieces of hexagonal patterns for fixed circle sizes, sometimes resulting in larger areas left unpacked because they might miss the tiniest gap to allow the circle in there. The fact that the a circle is locked in place once in the packing, often leaves large unpacked areas both in the plane and on surfaces in 3D space when using a narrow range of circle sizes. Thus having a wide range of circles sizes will often result in tighter packings as the algorithm has more freedom to fill in small areas.

Another limitation is that the algorithm require, by definition, tangent circle pairs to construct new circles. However, sometimes tiny gaps form and prohibits further expansion of the packing as was clearly shown by figure 19. This is mostly a problem on curved surfaces and is not as common in the plane.

4.2 Analytic vs. numeric computations

Having utilized both an analytic and numeric approach to solve the geodesic circle packing problem, their pros and cons are addressed in this section.

There is no doubt that analytic solutions to the geodesic problem are generally much better than numerical solutions, as computations of distances are much quicker and accurate given a closed formula. With that said, obtaining

analytic solutions is often a task that is too difficult to solve. In that case the numerical approach can be seen as a tool to obtain results regardless of complex geodesic equations.

It is important to emphasize, that obtaining analytic solutions is always better for the sake of computational resources when making geodesic circle packings. This case was made clear when making packings on the sphere. The analytic use of the stereographic projection made the implementation able to complete the algorithm within a few seconds. In contrast, the numeric implementation ran for nearly 10 minutes before completing the algorithm. This is unfortunately a general trend for the numerical implementation, using several minutes for all packings presented in this report. All packings made in section 3.2 have around 100-120 geodesic circles. In a similar time frame the analytic algorithm have been tested to pack more than 10000 circles.

As seen through use of the stereographic projection, it is sometimes possible to find alternative parametrizations of a surface, that maps euclidean circles in the parameter domain to geodesic circles on the surface itself, making the problem much simpler.

In conclusion, one should always strive to solve the problem analytically and use the numerical approach if it proves too difficult.

4.3 Periodic domains

A partly solved issue in this project is that of periodic domains. Domains may be periodic in one or both directions, allowing for "jumps" from one side of the domain to the other in an instant. This is the case for both the cylinder, sphere and torus. A way of fixing this problem is to keep copies of the packing shifted on either side of the domain and only add circles within the domain. This solution can be applied efficiently to the analytic case, by working modulo the length of the parameter interval. Thus this was handled well for the periodicity of u for the cylinder. Unfortunately, for the numeric computations, no efficient solution was found during this project, thus the packings made with this method have visual marks from the lack of periodic handling. The most obvious case of this is seen in figure 22b. All suggested implementations for the numeric case were too slow to be viable.

4.4 Using circles to visualize surfaces

Visualization of 2D surfaces living in 3D space is almost exclusively done in 2D, as it is often presented on a piece of paper or monitor. Plotting a surface and projecting it into the plane will in almost any case be a poor visualization. Therefore, 3D visualization software programs often use techniques such as shadowing, wireframe, contourlines, coloring or combinations of multiple methods to reflect the geometry of a surface.

A suggestion of this report is that geodesic circle packings may be used as another way of visualizing surfaces. With the circle being a well known geometric object to many people, it is reasonable to imagine that interpreting the shape of a surface would be easier, compared to other methods, when seeing how circles are deformed on it. A comparison of different visualization methods alongside using geodesic circles, is provided in figure 21.

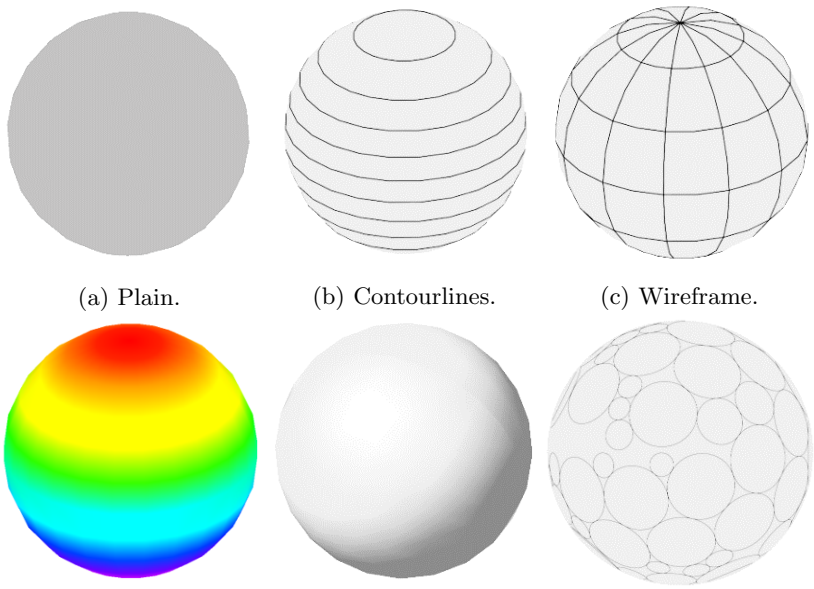

(a) Plain. (b) Contourlines. (c) Wireframe.

(d) Coloring. (e) Shading. (f) Geodesic circles.

Figure 21: Different visualizations of the sphere.

In section 3, geodesic circle packings were made on 4 different 2D surfaces in 3D space. All these surfaces may be inspected by only considering their geodesic circles. Such views are provided below in figure 22. As understanding of the geometry of a shape based on visual inputs is completely subjective and a matter of personal preference, nothing can be concluded in regards to the question of geodesic circle packings being better or worse for visualization.

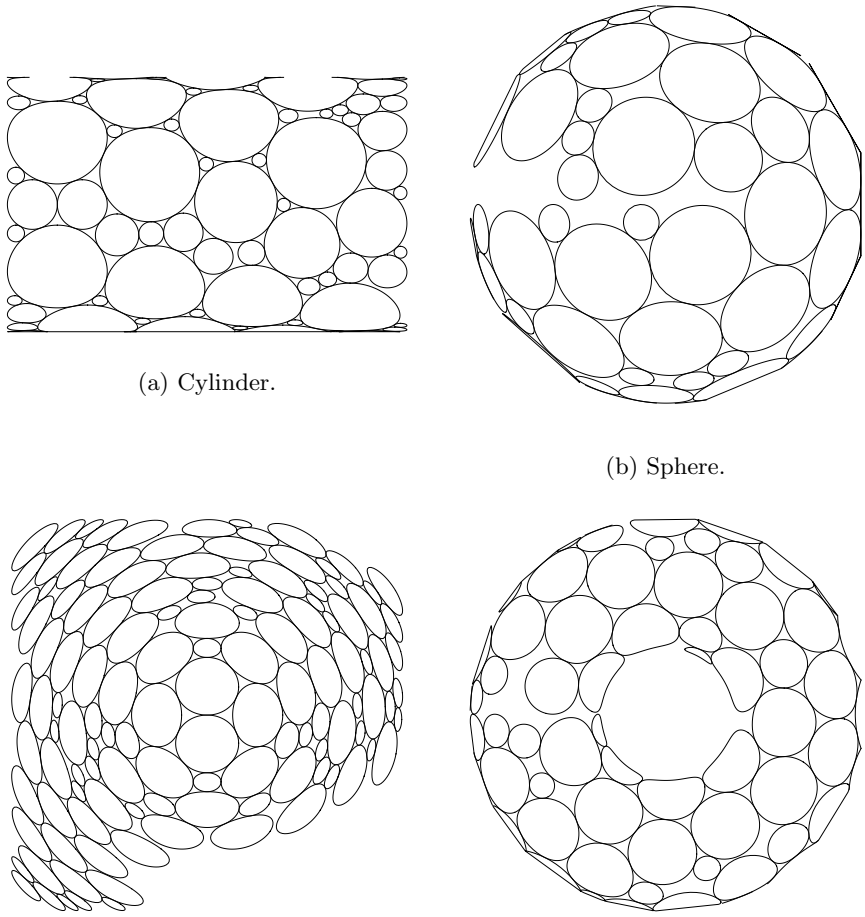

(a) Cylinder.

(b) Sphere.

(c) Quadratic.

(d) Torus.

Figure 22: Geodesic circle packings.

5 Conclusion

The main goals of this project was to setup a framework, for packing circles on 2D surfaces in 3D space using a tangent circle pair algorithm, and based on the theory make an implementation to do it in practice.

Initially, the algorithm was implemented in the plane. Then it has been explored how the concept of circles and circle packings can be generalized to arbitrary 2D surfaces in 3D space. This lead to the notion of general circles in metric spaces as point collections a fixed distance from a center according to any given metric. Wanting the circles on the surfaces to look as much like euclidean circles as possible, the generalization of straight paths, namely the concept of

geodesics, was explored along the theoretical framework for computing them.

The concept of geodesic distance was then used as a metric for general circles, and proved to make circles on surfaces that indeed resembles euclidean circles in the plane, so called geodesic circles.

Based on this, the geodesic equations was derived for a selection of surfaces, namely a cylinder, sphere, quadratic surface and torus. These equations proved difficult to solve in some cases, which lead to the development of a framework that can solve the problem numerically. While the implementation works, it has not yet been optimized and is rather slow compared to using analytic solutions.

As it is fast and somewhat easy to run the algorithm in the plane, it is suggested that geodesic circle packings can be made through maps that preserve circles in the parameter domain as geodesic circles on the surface itself, simplifying the problem by quite a margin. This idea was explored through use of the stereographic projection, which was proven to map circles in the plane to geodesic circles on the unit sphere.

In conclusion, the main goals of this project has been fulfilled.

6 Outlook

This section provides some ideas for continuations of this project.

Starting by addressing some of the issues of this project itself. As mentioned, the main problem left unsolved in this project, is the efficient handling of periodic domains in the numeric case. Solving this problem would fully complete the implementation. Then follows a task of optimizing both the analytic and especially the numerical implementation. At the moment, both implementations check all circles in the packing when trying to add new circles. As a result, they both suffer from running ever slower as the packing grows, essentially "drowning". In algorithmic terms they run in $O(N^2)$ time with N being the number of circles in the final packing. A suggestion is to organize the domain in smaller grids such that only circles in neighbouring grids are checked rather than all. Theoretically, this would solve the drowning problem completely and improve the runtime to $O(N)$.

Section 2.1 explain the concept of general circles in metric spaces. It would be interesting to investigate circle packings in the plane through use of different metrics. The p-norm for other values than 2 could be interesting as an example. For $p = 1$, circles would be 45 degree tilted squares, and thus one could perhaps use the algorithm in this setting to figure out how to tile different domains.

This report is exclusively using the tangent circle growing algorithm described in section 2.3. As seen, it sometimes struggle to find new tangent pairs to grow from, and packing circles of one size is generally not done well when the surface curves. However, there exist several algorithms for packing circles

in the plane, that can maybe also be generalized to 2D surfaces and applied to solve these issues. Some suggestions are the random circle growing algorithm implemented by "The Coding Train"[8] and physics assisted circle packing like grasshopper[9].

[8] https://www.youtube.com/watch?v=QHEQuoIKgNE
[9] https://www.youtube.com/watch?v=HvznxaBzQr4